

Special Article - Sugarcane Sustainable Production

Tribological Performance of Hardfaced/Thermally Sprayed Coatings for Increased Wear Resistance of Cutting Blades Used in Harvesting Sugarcane

Cooke KO^{1,2*}¹Faculty of Engineering and informatics, University of Bradford, UK²Department of Mechanical Engineering, University of Technology, Jamaica

*Corresponding author: Kavian O Cooke, Faculty of Engineering and informatics, University of Bradford, Richmond Road, BD71DP, UK, Department of Mechanical Engineering, University of Technology, 237 Old Hope Road, Jamaica

Received: March 07, 2019; Accepted: May 01, 2019;

Published: May 08, 2019

Abstract

Mechanical harvesters base-cutter blades used in the harvesting of sugarcanes require hard, wear-resistant surfaces capable of withstanding the harsh operating environment. This study evaluates the tribological performance of WC–FeCrCoNiTi coatings (97MXC), deposited by Electric Wire Arc Spraying (EWAS), as a potential candidate for producing wear resistant surface for mechanical harvester base-cutter blades. The coatings were characterized for hardness, microstructure and abrasive wear resistance under both laboratory and field-testing conditions. The results show that the difference in hardness of the coatings was significantly affected by the spraying parameters and optimization of these variables to maximize coating hardness enhances the tribological performance of the coating. Field testing of the optimized coatings confirms that the 97MXC coating deposited by EWAS had the ability to significantly extend the cutting life of blades used in the harvesting sugarcane.

Keywords: Thermal spay coatings; Oxide content; Abrasive wear; Porosity; Optimization

Introduction

Wear can have deleterious effects on equipment engaged in sliding, rolling or reciprocating motion within the agricultural sector. These effects have always been a costly but an unavoidable part of all agricultural operation and maintenance [1]. Since agricultural equipment is subject to extreme operational conditions, they require adequate surface protection against corrosion and mechanical wear. As such, users of field equipment are demanding extended service life and reduction in the frequency of maintenance. Achieving this goal requires a systematic appraisal of the components under operating conditions to determine the failure modes that limit service life. By this appraisal system, it is possible to identify solutions to the problem. In sugarcane harvesting, mechanical harvester base cutter blades are used to cut sugar cane plants at the ground level, before it is moved to the chopper drum where it is further chopped into billets with which the trucks are loaded for delivery to the factory.

Base cutter blades present many inconsistencies in their ability to resist wear. These inconsistencies mainly involve frequent dulling of the cutting edge and sometimes fracture Figure 1 when the blades hit against extraneous matters such as stones, and sand. A problem shared by many sugar producing countries.

The wear process encountered by base-cutter blades is very complex with a large number of variables that may influence how the material behaves under different conditions. These include type and mode of loading, interaction rate and time, component geometry, materials properties, and environmental factors. As such, friction and wear are not determined solely by the properties of the material but by the characteristics of the entire engineering system. Wear-resistant materials are hard and have low values of toughness, making

fabrication difficult and expensive. On the other hand, since wear is a surface phenomenon the use of an appropriate surface layer may have a significant effect and therefore the application of thermal spray coatings or other surface treatments are most attractive.

While several methods are available for engineering surfaces with the required properties. These technologies are often expensive and uneconomical. One of the most attractive methods of minimizing the wear of equipment is by the application of surface treatment techniques. Among a large number of existing surface treatment techniques, thermal spraying is one of the most widely used to improve the wear behavior of various engineering components [2-4]. While there are several variants of thermal spraying utilizing different heating sources or protective gases the general principle of operation remains the same. A feedstock material is melted and propelled as atomized particles or droplets onto a surface by a suitable

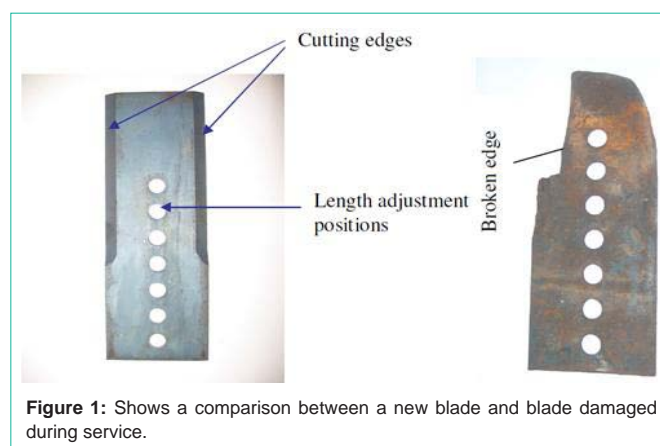


Figure 1: Shows a comparison between a new blade and blade damaged during service.

Table 1: Chemical composition of the materials used in this study (wt. %).

Materials	C	WC	Ni	Ti	Cr	Fe	Co	Mn	Si
97MXC	-	45	4	2.5	11	30	7.5	-	
Substrate	0.4	-	-	-	0.9	Bal.	-	0.95	0.29

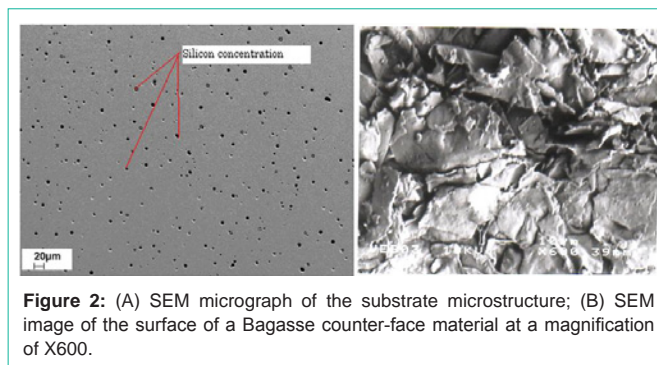
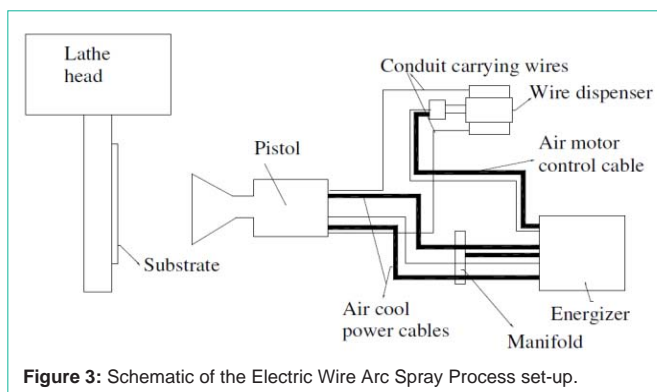
Table 2: Parameters used to evaluate the wear performance of the optimized coating.

Parameters	Effect of Load	Effect of Speed
Speed (rpm)	100	Varied 100 - 500
Load (N)	Varied 10 - 40	20 N
Sliding distance (m)	1000	1000
Abrasive particle	SiO ₂	SiO ₂
Mass flowrate of SiO ₂ (g/s)	6	6

compressed gas. The impact of the particle with the substrate causes the particles to flatten to form a coating. The high-velocity impact and rapid solidification of the melted particles form cohesively bonded splats ranging in size from 10-100 μm [2]. The physical properties of the deposits will depend on the cohesive strengths between the splats, the size, and morphology of the porosity, the presence of cracks and defects within each coating layer [5]. Coatings use in harsh environmental conditions typically metal alloys containing hard particles such as WC [6], CrC [7] or TiN particles embedded into a ductile matrix. The function of the particle is to provide structural reinforcement and support because of its high Young's modulus and hardness, while the matrix is made from soft metals such as Co, Ni, Fe or various alloys of these elements and protects the particle from environmental degradation and reduce internal stress within the coating.

A popular technique used for producing hard, wear resistant surfaces is the High-Velocity Oxyfuel (HVOF) spraying. This process is based on the supersonic jets achieved by the expansion of the products of combustion between oxygen and fuel passing through a convergent-divergent nozzle. The high deposition rate and efficiency and the lower spray temperature make such processes a reliable solution for producing dense and oxide-free coatings. However, the equipment required for the process is expensive [8,5].

Among the available thermal spray process EWAS is a cost-effective method of modifying the surface properties of agricultural tools to withstand surface degradation in harsh environments [9,10]. EWAS requires the formation of an arc between two consumable electrodes which melts the material. High-pressure air is used to propel the melt toward the substrate which splats to form a layered coating on the surface of the substrate. The use of air in the process, however, can lead to oxidation of the particles during flight, which, has the potential to affect the amount of porosity observed in the deposited coating. The scientific literature shows that a direct correlation exists between the hardness of EWAS coatings and the porosity of the coatings [11]. Additionally, considering the inverse relationship that exists between wear rate and the hardness of the material as illustrated by the Archard wear equation. It is essential to fabricate coatings that have both high hardness and low porosity. Previous studies on EWAS have shown that coating hardness and porosity are strongly influenced by spray parameters such as spray distance, current, voltage and air pressure [12]. On this basis, it is

**Figure 2:** (A) SEM micrograph of the substrate microstructure; (B) SEM image of the surface of a Bagasse counter-face material at a magnification of X600.**Figure 3:** Schematic of the Electric Wire Arc Spray Process set-up.

critical that the settings of each parameter are selected in a way that maximize the coating hardness and minimize the porosity of the coating. One method of identifying the appropriate setting of the parameters is through statistical optimization. One approach is to optimize the parameters using Taguchi L9 since the technique minimizes the number of experiments to be conducted.

This study provides a comprehensive assessment of the tribological performance of the WC-FeCrCoNiTi (Praxair model name - 97MXC) coatings deposited by EWAS. The spray parameters were optimized to maximize coating hardness. The wear behavior of the optimized coatings was assessed under both laboratory conditions and in-service testing. The Taguchi L9 design of experiment was used to optimize spray parameters of the EWAS equipment. A comparative analysis of the wear performance of the optimized coating and the as-received cutting blades used in the harvesting of sugar cane is also presented.

Materials and Methods

The composition of the materials used in this study is presented in Table 1. The wear assessment was divided into two parts: laboratory testing and field testing. For the laboratory testing, samples of dimensions 50mm x 30mm x 10mm were cut from the as-received blades and the surfaces prepared for coating. Prior to arc spraying, the surface of the substrates were grit blasted with alumina particles and cleaned with acetone. The microstructure of the substrate is shown in Figure 2(A&B). The spray material was WC-FeCrCoNiTi wire of 1.6mm diameter and chemical composition as shown in Table 1 and carries a code name 97MXC.

The final coating thickness was maintained within a range of $250\mu\text{m} \pm 0.5\mu\text{m}$. The deposition process was carried out using a

Table 3: Experimental factors and their levels.

Levels	Pressure (bar)	Voltage (V)	Current (A)	Distance (mm)
1	3.5	30	150	80
2	4.5	35	175	100
3	5.0	40	200	120

Table 4: Experimental factors and the level of each factor studied.

Experiments	Pressure (bar)	Voltage (V)	Current (A)	Distance (mm)	Hardness	Porosity
1	1	1	1	1	828.55	8.03
2	1	2	2	2	941.81	8.75
3	1	3	3	3	647.37	7.83
4	2	1	2	3	755.13	10.07
5	2	2	3	1	635.19	10
6	2	3	1	2	892.45	9.2
7	3	1	3	2	961.53	5.96
8	3	2	1	3	847.36	13.02
9	3	3	2	1	670.03	8.79

Table 5: Properties of the optimized coating.

Coating	Thickness (µm)	Porosity (Vol %)	Hardness	Oxide size (µm)	Density (g/cm ³)
97MXC	167	3.6	1158.47	4.5	5.9

240 Twin wire arc spraying machine supplied by Metallization Ltd (West Midlands, United Kingdom). Samples were positioned for coating as shown in Figure 3. The spray parameters such as spray distance, current, voltage, and air pressure were chosen as variables for the present study. Nine experiments were conducted according to Taguchi L9 design of experiments and three coatings were developed for each experiment.

The microstructure of the as-deposited coatings was examined using an Aspx scanning electron microscopy (Model 309, RJI Micro and Analytic, Karlsruhe-Nuethaud, Germany). The chemical composition of the coatings was evaluated using an Energy Dispersive x-ray Spectroscopy (EDS) system attached to the SEM. The specimens were prepared for microstructural evaluation using standard metallographic preparation techniques. Optical porosity measurements were made in accordance with ASTM E2109 - 01(2014). Porosity measurements were performed on the cross-section of the coatings using a Zeiss optical microscope A Mitutoyo Vicker's micro-hardness tester at a load of 0.1kg was used to evaluate the hardness of the coatings and the as-received blades. Micro-hardness tests were performed on the cross-section of the coatings according to ASTM E92 standard test method for a Vickers micro-hardness testing. Indentations were made using a diamond-shaped indenter to which the load was applied for 30s. Wear tests were carried out on the optimized coating in two stages, laboratory testing and field testing. Laboratory testing was conducted on a Plint multi-station block-on-ring tribo-tester using the test parameters shown in Table 2. The coatings were subjected to a 30-minutes wear test during which a bagasse board of dimensions 97 mm diameter × 25 mm wide was used as the counter-face material. An SEM image of the surface of the bagasse board is shown in Figure 2(B). Each sample was weighed before and after testing using an Adventurer (OHAUS Europe

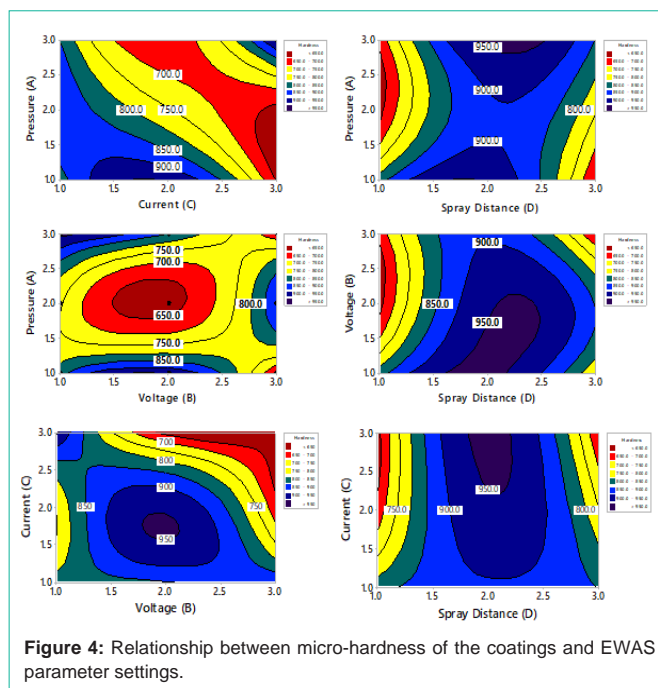


Figure 4: Relationship between micro-hardness of the coatings and EWAS parameter settings.

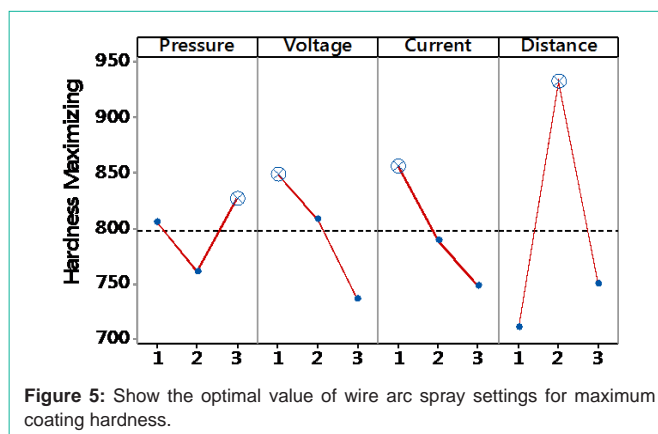


Figure 5: Show the optimal value of wire arc spray settings for maximum coating hardness.

GMBH, Greifense, Switzerland) electronic scale with an accuracy of 0.0001g. To ensure repeatability three specimens were tested for each condition. The coatings were subjected to three-body abrasive wear tests by flowing SiO₂ sand between the bagasse disc and the test sample at a flow rate of 6.0g/s.

Design of Experiments

Prior to wear testing, the parameters of the electric wire arc spray process were optimized to maximize coating hardness using a Taguchi L9 Design of Experiments (DOE). This approach is an effective tool since it reduces the number of experiments to be conducted. The level of each factor studied are presented in Table 3. The levels were set based on preliminary experimental study and previous work [12]. The Taguchi L9 orthogonal array is shown in Table 4.

Results and Discussion

Contour plots: Influence of spraying parameters

The parameters of the electric wire arc spray machine were optimized to deposit the WC-FeCrCoNiTi wire. The relation between

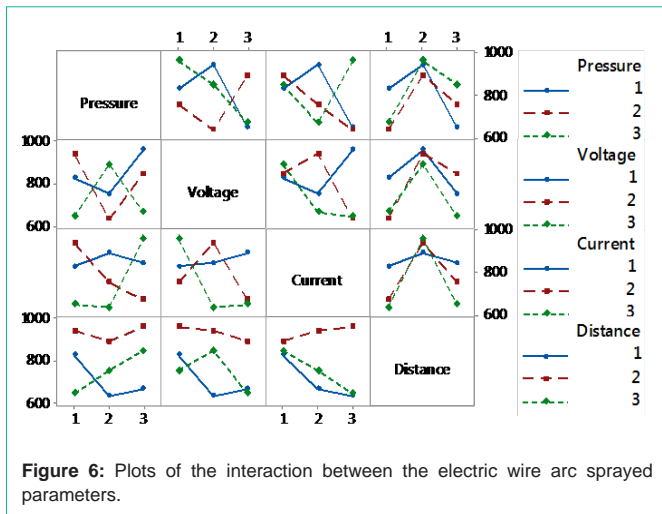


Figure 6: Plots of the interaction between the electric wire arc sprayed parameters.

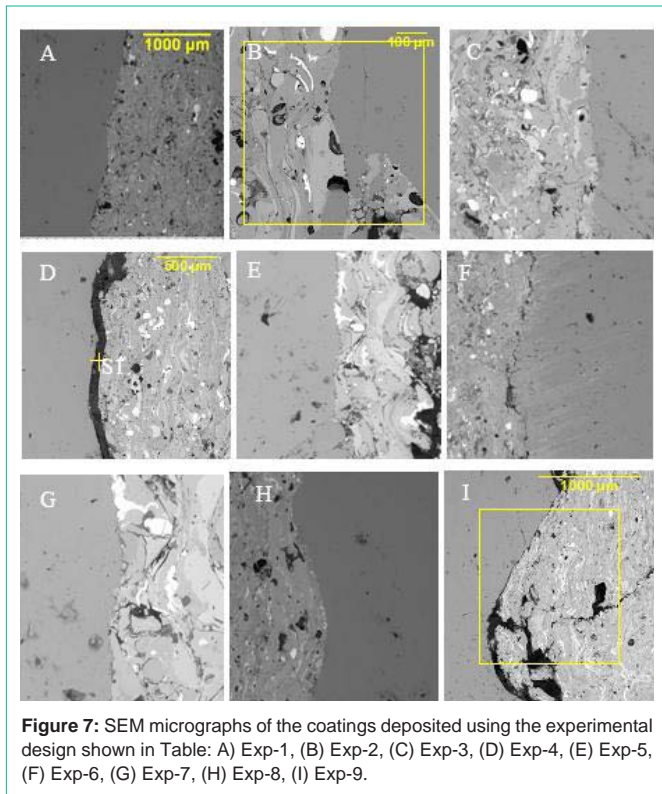


Figure 7: SEM micrographs of the coatings deposited using the experimental design shown in Table: (A) Exp-1, (B) Exp-2, (C) Exp-3, (D) Exp-4, (E) Exp-5, (F) Exp-6, (G) Exp-7, (H) Exp-8, (I) Exp-9.

the micro-hardness and the parameter setting are presented in Figure 4. The contour maps show the influence of current, voltage, pressure and spray distance on the coating hardness. The plots also allow for the prediction of hardness within any region of the experimental domain. The dark-colored regions of the maps indicate regions of higher hardness. The color distribution shown on the maps also confirms the complex interactions that exist between the electric wire arc spray parameters and the mechanical performance of the coatings.

Optimization of spraying parameters

Figure 5 shows a plot of the relationship between the spray parameters and the coating hardness. The objective of the optimization process is to find the best parameters set points that maximize

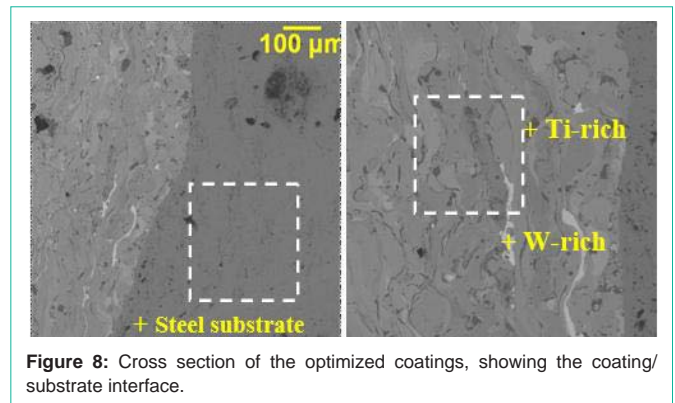


Figure 8: Cross section of the optimized coatings, showing the coating/substrate interface.

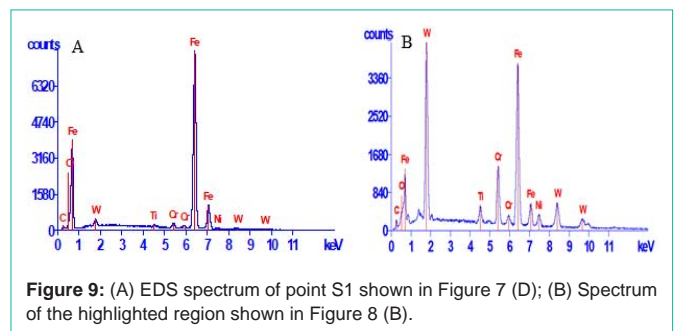


Figure 9: (A) EDS spectrum of point S1 shown in Figure 7 (D); (B) Spectrum of the highlighted region shown in Figure 8 (B).

coating hardness. According to the Archard’s wear equation, an inverse proportional relationship exists between wear rate and the hardness of the surface. Accordingly, higher surface hardness should correspond to lower wear rates. From the results presented in Figure 5, the coating hardness can be maximized if the following settings are used: pressure–level 3, Voltage–level 1, current–level 1 and spray distance–level 2. An analysis of the interaction between the parameters is presented in Figure 6 and show the complexity of the interactions between the factors and the level setting. If spray distance is held constant at level-2 coating, hardness can be maximized for all settings of the other three parameters. A positive correlation was found between; level-1 settings of current and voltage, the level-3 setting of pressure and level-2 setting of spray distance.

Verification experiment

The confirmation experiment was conducted from the optimal parameter settings presented in Figure 5. The results show that the coating hardness can be maximized if the following settings are used: pressure–level 3, Voltage–level 1, current–level 1 and spray distance–level 2. The properties of the optimized coating are shown in Table 5 and confirm that when the optimized parameters are used the coating hardness increased by 20% above the maximum coating hardness recorded for experiment 7 as shown in Table 4 from 961HV 0.1kg to 1159HV 0.1kg. These values are significantly greater than the 456HV 0.1kg recorded for the as-received base-cutter blades. In keeping with the increase of the coating hardness, the volume of porosity recorded with the optimized sample decreased when compared to the porosity data presented in Table 4. This behaviour is supported by the literature, which shows that an inversely proportional relationship exists between coating porosity and hardness [11].

Microstructural analysis

The SEM micrograph of the as-deposited coating for each of

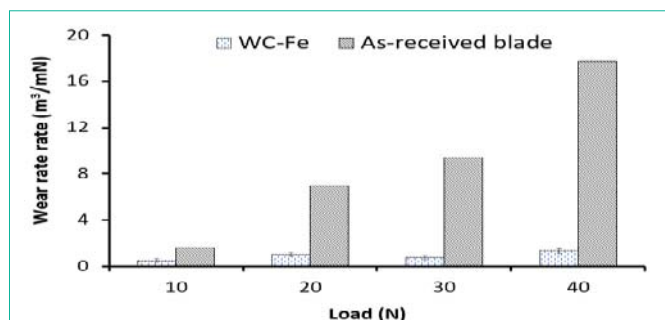


Figure 10: Specific wear rate as a function of load.

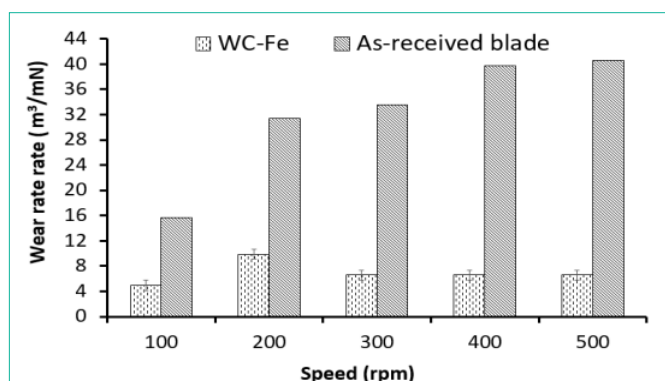


Figure 11: Effect of speed on the specific wear rate.

the nine experiments is presented in Figure 9 and revealed that the coating appeared to be dense with some porosity observed at the interface between the coating and the substrate. The coating deposited in experiment-6 experienced extensive cracking along the interface. While coatings produced in experiment-4 and experiment-9, experience the formation of an oxide layer between the substrate and the coating. EDS analysis of the compound suggests the formation of Fe_2O_3 . The dark spots throughout the coatings are pores or inclusion deposited into the coating during the spray process. A measure of the size of the dark spots found to be oxide particles found a significant variation of the percentage porosity/inclusion for each of the coating produced from the experimental runs. A summary of the percentage of porosity/inclusion is presented in Table 4.

When these coatings are compared to the microstructure of the optimized coating presented in Figure 7 & 8. The layers of the coatings are visible and show good adhesion between the coating and the substrates as well as between successive layers of the coating. In thermal spraying, particle deformation is necessary for the coating to coalesce, therefore, the deposition of coatings containing large carbides particles can result in the formation of void spaces where the particles have failed to amalgamate with surrounding particles. EDS analysis of the optimized coating showed that the grey areas are Ti-Rich phases which the white areas are WC-rich areas Figure 9. The absence of porosity/inclusion from the optimized coatings is attributed to a better interaction between the spray parameters that prevented large pieces of wire burn-offs from being deposited into the coatings. The microstructure of the as-received base cutter blades is presented in Figure 2. The EDS analysis of the as-received sample showed that the materials is a medium carbon steel containing

0.4wt% C and high silicon concentration within the dark spots shown in Figure 2.

Three-body abrasive wear behavior of the optimized coating

The wear behavior of the optimized coating was further evaluated under laboratory conditions to determine the effect of load and speed on the wear rate of the coatings and compared to the performance of the as-received blades.

Effect of load on the wear rate: The optimized coating was subjected to wear testing for 5000 cycles while the load was varied from 10N to 40N. The same number of cycles were used for each load setting. The specific wear rate of the surfaces was also evaluated as a function of sliding distance and applied load using Equation 1.

$$\text{Specific wear rate (K)} = \frac{V}{D_s L} \text{-----Equation 1}$$

If Equation 1 is substituted into Equation 4, the final equation for the specific wear rate can be written as shown in Equation 5.

$$\text{Specific wear rate (K)} = \frac{V}{D_s L} = \frac{M}{\rho D_s F} \text{-----Equation 2}$$

where M is the mass loss, ρ is the density, D_s is the sliding distance and F is the applied load.

A summary of the effect of load on the wear behavior of the substrate is presented in Figure 10(A) and shows that the specific wear rate of the substrate increased progressively with increasing load from $1.63\text{m}^3/\text{mN}$ at 10N to $17.74\text{m}^3/\text{mN}$ at 40N. On the other hand, the results showed that the wear rate of the WC-FeCrCoNiTi coating marginally increased from $0.49\text{m}^3/\text{mN}$ at 10N to $1.03\text{m}^3/\text{mN}$ at 20N, when the load was increased beyond 20N the wear rate fluctuated between $0.78\text{m}^3/\text{mN}$ and $1.33\text{m}^3/\text{mN}$ at 40N. The differences in the wear behavior of the coating and substrate can be attributed to higher hardness of the coating due to the presence of WC carbide particles in the coating.

Comparing the data to the scientific literature it was seen that specific wear rate is often seen as a material constant as long as the changes in the sliding distance and the contact pressure do not change to a great extent [13]. While the specific wear rate of the as-received blades appeared to be consistent which the published literature, while the WC-NiTiCrFeCo showed significant fluctuations as the load was increased. The differences in observed in the specific wear rate of the coating were attributed to the differences recorded in the materials properties such as; density, hardness, and porosity [14,15].

Effect of speed on the wear rate: The effect of speed on the as-received blade is shown in Figure 11 and indicated that as the speed is increased from 100rpm to 200rpm, the specific wear rate increased from $15.68\text{m}^3/\text{mN}$ to $31.37\text{m}^3/\text{mN}$. Similarly, when the speed is increased beyond 200rpm the specific wear rate increased progressively to $39.79\text{m}^3/\text{mN}$ at 500rpm. When the speed was increased incrementally to 500rpm, the specific wear rate change marginally to $40.61\text{m}^3/\text{mN}$.

When compared to the 97MXC coating shown in Figure 11. The results show that when the speed is increased from 100rpm to 200rpm, the wear rate increased from $4.93\text{m}^3/\text{mN}$ to $9.86\text{m}^3/\text{mN}$ respectively. However, when the speed is increased beyond 200rpm the specific wear rate decreased to $6.58\text{m}^3/\text{mN}$ and remain constant while the

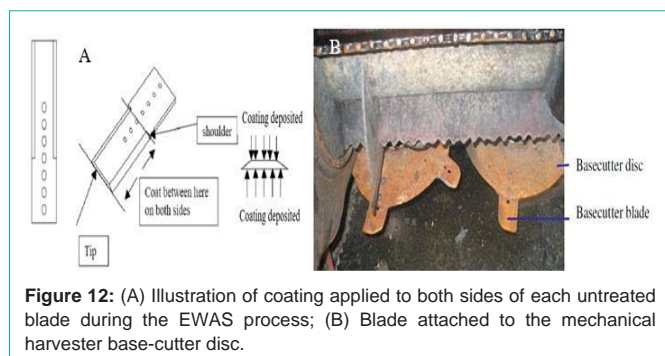


Figure 12: (A) Illustration of coating applied to both sides of each untreated blade during the EWAS process; (B) Blade attached to the mechanical harvester base-cutter disc.

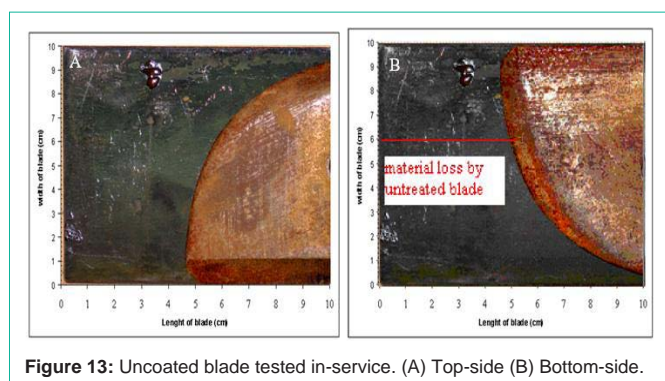


Figure 13: Uncoated blade tested in-service. (A) Top-side (B) Bottom-side.

speed is increased incrementally to 500rpm. Analysis of the wear data suggests that the coated samples provided better wear resistance than the as-received blades. The better wear resistance of the coating was attributed to the higher hardness and density of the coating.

Field testing: Field testing of the optimized coating was performed to confirm the results collected under laboratory conditions. The coated blades were bolted to the base-cutter disc as shown in Figure 12. Five coated blades were bolted to disc A and five uncoated blades were bolted to disc B. The blades were operated in the field environment for seven days after which the blades were removed and the volume and mass loss recorded.

Figure 13 shows the edges of the as-received base-cutter blade after the testing period which indicates that a significant volume of the blade was lost during operation. Examination of the images shown in Figure 8 revealed that the untreated blades experienced extensive mass loss over the test period. A comparison of the blades test showed that the untreated blades had the highest cumulative mass loss and hence the shortest life span. Over the test period, the untreated blade lost approximately 228g from its mass and along its cutting edge. Additionally, the edges of the blades appeared to be rounded, which could reduce its ability to effectively carry out any further cutting action. When compared to the EWAS coated blade shown in Figure 14, the coated blades experienced a mass loss of 96g, while the dimensions of the blade changed by approximately 0.5cm from its length, the untreated blades lost approximately 5cm from its length. This difference in wear rates could be attributed to the enhanced hardness of coated samples. Hardness is considered to be a property of a material which can significantly affect the wear rate of frictional components and is directly affected by the microstructure and porosity of the materials. By comparing the Relative Wear Resistance

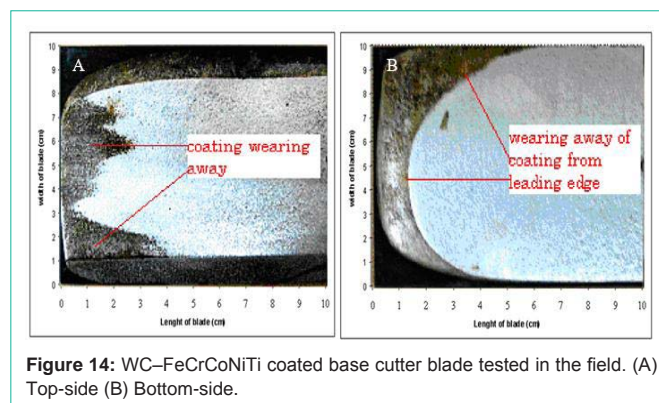


Figure 14: WC-FeCrCoNiTi coated base cutter blade tested in the field. (A) Top-side (B) Bottom-side.

(RWR) of the as-received blades and the EWAS coated blades using the mass loss it was found that the coated blades are 2.4 times more wear resistant than the uncoated blades as shown in Equation 3. The improved tribological performance of the cutting blades when coated with EWAS WC-FeCrCoNiTi is expected to decrease the overall cost replacing base-cutter blade to the sugar industry by approximately 50%.

$$RWR = \frac{\text{mass loss of untreated blade}}{\text{mass loss of coated blade}} = \frac{228 \text{ g}}{96 \text{ g}} = 2.4 \text{ -----Equation 3}$$

Conclusion

This study was conducted to evaluate the tribological performance of 97MXC deposited by electric wire arc spraying. The results showed that the parameters of the of the EWAS process can be effectively optimized using the Taguchi orthogonal array.

Optimization of the process parameters led to the development of coatings with reduced porosities and increase hardness. Microstructural analysis of the optimized coating showed that the layers of the coatings are visible with good adhesion between the coating and the substrate as well as between successive layers of the coating.

Laboratory testing of the optimized coating showed that the 97MXC coating were capable of withstanding the harsh operational conditions under which base-cutter blades operate. Field testing confirmed that these materials are capable of doubling the cutting life of base-cutter blades used in the harvesting of sugarcane which should lead to approximately 50% savings on the cost to replace base-cutter blades and the accompanying downtime experienced during sugarcane harvesting.

References

1. Szymański K, Hernas A, Moskal G, Myalska H. Thermally sprayed coatings resistant to erosion and corrosion for power plant boilers - A review. *Surf Coatings Technol.* 2015. 268: 153-164.
2. Fauchais P, Vardelle A. Thermal Sprayed Coatings Used Against Corrosion and Corrosive Wear. In *Advanced Plasma Spray Applications.* 2012.
3. Geaman V, Pop MA, Motoc DL, Radomir I. Tribological Properties of Thermal Spray Coatings. 2013.
4. Dorfman MR, Sharma A. Challenges and Strategies for Growth of Thermal Spray Markets: The Six-Pillar Plan. *J Therm Spray Technol.* 2013.
5. Picas JA, Punset M, Baile MT, Martín E, Forn A. Properties of WC-CoCr based coatings deposited by different HVOF thermal spray processes. In *Proceedings of the Plasma Processes and Polymers.* 2009.

6. Hinners H, Konyashin I, Ries B, Petrzik M, Levashov EA, Park D, et al. Novel hardmetals with nano-grain reinforced binder for hard-facings. *Int J Refract Met Hard Mater*. 2017.
7. Espallargas N, Berget J, Guilemany JM, Benedetti AV, Suegama PH. Cr₃C₂-NiCr and WC-Ni thermal spray coatings as alternatives to hard chromium for erosion-corrosion resistance. *Surf Coatings Technol*. 2008.
8. Bolelli G, Börner T, Milanti A, Lusvarghi L, Laurila J, Koivuluoto H, et al. Tribological behavior of HVOF- and HVOF-sprayed composite coatings based on Fe-Alloy + WC-12% Co. *Surf Coatings Technol*. 2014.
9. Oliver G, Buchanan V, Cooke K. A tribological study for an increased coefficient of friction in the extraction of sugarcane juice. *Tribol Trans*. 2007.
10. Tian H, Wang C, Guo M, Tang Z, Wei S, Xu B. Influence of Ni and Cr on the high-temperature wear resistance of FeNiCrAl coatings. *Results Phys*. 2019; 12: 959-969.
11. Şerban VA, Roşu RA, Bucur AI, Pascu DR. Deposition of titanium nitride layers by electric arc-reactive plasma spraying method. *Appl Surf Sci*. 2013.
12. Cooke K, Oliver G, Buchanan V, Palmer N. Optimisation of the electric wire arc-spraying process for improved wear resistance of sugar mill roller shells. *Surf Coatings Technol*. 2007; 202: 185-188.
13. Friedrich K, Schlarb AK. *Tribology of Polymeric Nanocomposites: Friction and Wear of Bulk Materials and Coatings*. Tribol Interface Eng Ser. 2008.
14. Kuforiji C, Nganbe M. Modelling the effects of microstructure, properties and abrasion conditions on the wear resistance of SS316L-Al₂O₃composites. *Tribol Int*. 2017.
15. Jin C, Onuoha CC, Farhat ZN, Kipouros GJ, Plucknett KP. Microstructural damage following reciprocating wear of TiC-stainless steel cermets. *Tribol Int*. 2017.